

## Nucleation: What Happens at the Initial Stage?\*

Tian Hui Zhang and Xiang Yang Liu\*

Nucleation, a process taking place on a nano- or sub-nanoscale in typical atomic and molecular systems, creates original crystal embryos from the mother phase. It is one of the most important aspects in our daily life. It is important in situations ranging from the condensation and freezing of water (e.g. rain, snow, freezing),<sup>[1]</sup> the formation of bones and teeth and the correlation between synergetic structures and their superior properties,<sup>[2]</sup> to semiconductor/IT and nanotechnologies,<sup>[3,4]</sup> because in most cases nucleation determines whether a phase will form, how the formation will occur, and what structure will be formed.<sup>[5,6]</sup> Therefore, it is the cornerstone for many very important modern technologies, including life/nanosciences and engineering. Although many different nucleation theories, both classical and nonclassical, have been developed, nucleation, in particular its mechanism, continues to be one of the most poorly understood and disputable phenomena in the past half century.<sup>[7–9]</sup>

The formation of nuclei is essentially a dynamic process dominated by the competition between the reduced bulk free energy and the increased surface free energy. This competition gives rise to the so-called nucleation barrier and the critical size of nuclei. One of the major issues in the theoretical study of nucleation is to determine the nucleation barrier. However, the nucleation barrier is dependent on the structure of nuclei as well as on supersaturation. The so-called classical nucleation theory (CNT),<sup>[7,8]</sup> which is the most widely used theory about nucleation, assumes that the structure and hence the surface tension of nuclei are the same as that of the new stable phase. Nevertheless, this assumption has been challenged by evidence from simulations<sup>[10–12]</sup> and experiments.<sup>[13–15]</sup> The key point of this evidence is that in crystallization, nucleation begins with a metastable structure and the stable structure is reached subsequently. This picture is consistent with the prediction of the Ostwald's rule.<sup>[16,17]</sup> However, the kinetics of the transition from the metastable structure to the stable structure has so far been unclear because of the absence of direct observation of the transition

process in real space. This is because in typical atomic systems, atoms are too small to be observed directly. As an alternative approach, colloids have been employed as a model system to study phase transitions,<sup>[16,21]</sup> because colloidal particles in solutions behave like large “atoms”,<sup>[18,19]</sup> and the phase behavior of colloidal suspensions is similar to that of atomic and molecular systems.<sup>[20]</sup> The advantage of this kind of model system is that colloidal particles, and thus the nucleation process, can be observed directly by a normal optical microscope. Furthermore, the thermodynamic driving force for the nucleation can be controlled precisely in colloids, so that quantitative measurement and data interpretation become possible.<sup>[18,19]</sup>

In this study, the structure evolution of nucleating clusters at the initial stage of nucleation was examined in a two-dimensional colloidal model system driven by an alternating electric field. It was found that distinct from the assumption of the CNT, nuclei are created with a metastable liquid-like structure, and the final stable crystal-like structure is approached through a continuous structure transition. This study offers the first experimental observation of the structure transition. Furthermore, the impact of the metastable structure on nucleation barrier was investigated in a quantitative manner. As two-dimensional (2D) and three-dimensional (3D) nucleation kinetics are very similar,<sup>[23]</sup> the knowledge acquired in this study will significantly advance our understanding of nucleation in general.

Figure 1a shows the experimental setup, and Figure 1b shows the phase diagram of the solution used in this study. Three different phases were identified: three-dimensional liquid (3DL), two-dimensional crystal (2DC), and three-dimensional disordered aggregate (3DDA). In the 2DC region, the attractive force between the colloidal particles will be enhanced by increasing the amplitude or decreasing the frequency of the alternating electric field (AEF).<sup>[21,22]</sup> To quantify the ordering of the two-dimensional crystal nuclei, a local two-dimensional bond-order parameter was defined by Equation (1).

$$\psi_6(r_i) = M^{-1} \left| \sum_j e^{i6\theta_{ij}} \right| \quad (1)$$

Here,  $r_i$  is the center of particle  $i$ , and  $\theta_{ij}$  is the angle subtended between the vector from particle  $i$  to its  $j$ th nearest neighbor and the arbitrarily chosen  $x$  axis.  $M$  is the number of nearest neighbors of particle  $i$ . Positions of particles in a nucleus were extracted by an image processing program developed in house. The average minimum of the center-center distance  $d$  between two particles was measured, and  $1.5d$  was used as the cutoff value in determining the nearest neighbors. A value of 0.8 for  $\langle \psi_6 \rangle$  in a typical crystalline

[\*] Prof. X. Y. Liu  
MIT-Singapore Alliance, Department of Physics  
National University of Singapore  
2 Science Drive 3, Singapore 117542 (Singapore)  
Fax: (+65) 6777-6126  
E-mail: phyluxy@nus.edu.sg

Dr. T. H. Zhang  
Van't Hoff Laboratory for Physical and Colloid Chemistry  
Debye Institute, Utrecht University  
Padualaan 8, 3584 CH Utrecht (The Netherlands)

[\*\*] This research is supported by ARF Project R-144-000-148-112. We are much indebted to Dr. C. Strom for her valuable suggestions and critical reading of the manuscript.

Supporting information for this article is available on the WWW under <http://dx.doi.org/10.1002/anie.200804743>.

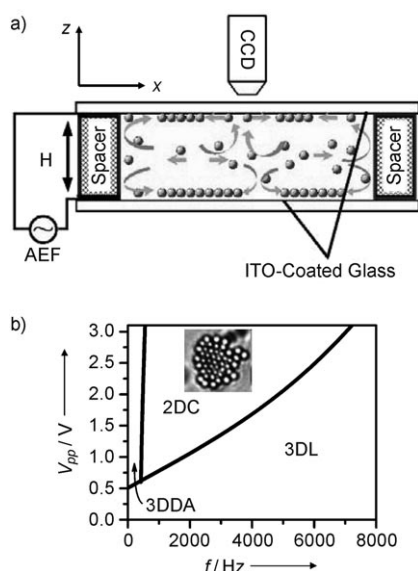


**Figure 1.** a) Experimental setup: A colloidal suspension is sealed between two ITO-coated conducting glass plates separated by insulating spacers. The gap between the two glass plates is  $H = 120 \pm 5 \mu\text{m}$ . The dynamic process is recorded by a digital camera (CCD) for analysis. AEF = alternating electric field. b) Phase diagram of the system when the concentration of  $\text{Na}_2\text{SO}_4$  is  $2 \times 10^{-4} \text{ M}$ .  $V_{\text{pp}}$  = peak-to-peak voltage.

structure was used as the criterion for defining a crystal-like nucleus.

Figure 2 shows a typical process of nucleating a crystal nucleus under the conditions  $V_{\text{pp}} = 2.5 \text{ V}$  and  $f = 5000 \text{ Hz}$ . Figure 2a suggests that the initial structure of the nucleus is liquid-like. In the subsequent growth, its core first becomes ordered, but the outer layer remains liquid-like (Figure 2b).

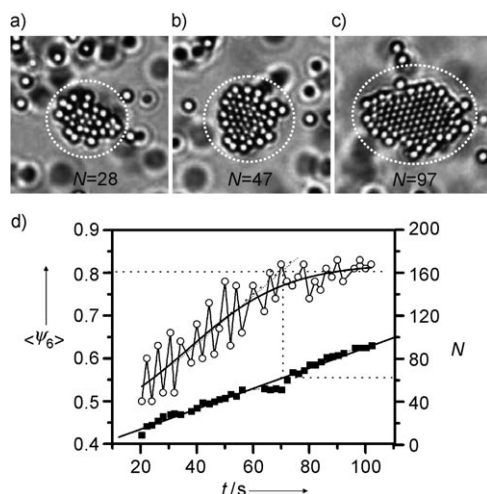


**Figure 2.** Structural evolution of nuclei under conditions of  $V_{\text{pp}} = 2.5 \text{ V}$ ,  $f = 5000 \text{ Hz}$ . a) The initial structure of nuclei is liquid-like. b) As the nucleus grows, its core first becomes ordered and the exterior layer remains liquid-like. c) The nucleus becomes completely ordered after the size exceeds a critical value. d)  $\langle \psi_6 \rangle$  ( $\circ$ ) and  $N$  ( $\blacksquare$ ) as a function of time. Particles in this system are illustrated by the diffracted light. The screening of particles to each other makes the particles in the core of the nuclei look smaller than those in the outer layer.

The nucleus becomes entirely crystal-like and grow spontaneously only when it is big enough (Figure 2c). To quantify the structure evolution,  $\langle \psi_6 \rangle$  was measured as a function of the nucleus size  $N$ . From Figure 2d, we can see that as the size of the nucleus increases with time and that  $\langle \psi_6 \rangle$  increases gradually at the early stage and reaches a plateau of approximately 0.8 as the size exceeds 70. Before the plateau, the increase of the value of  $\langle \psi_6 \rangle$  could be fit as a linear function of time. The size corresponding to the intersection point of the fitting line and the horizontal line of  $\langle \psi_6 \rangle = 0.8$  is identified hereafter as the transition size  $N_{\text{trans}}$ . The nuclei can grow spontaneously with a stable crystal-like structure only when they are larger than  $N_{\text{trans}}$ . In this observation, the initial structure of the crystal nuclei is different from its final stable structure, and the crystallinity of the nuclei is size-dependent. The structure transition from liquid-like to the final crystal-like structure is a continuous process in terms of the order parameter. This result is in conflict with the assumption of the CNT.

The behavior of  $\langle \psi_6 \rangle$  and  $N$  as a function of time, however, may be different for different individual growing nuclei: some nuclei may grow much faster than other nuclei. Furthermore, since the electric field in the solution is not perfectly homogeneous,  $N_{\text{trans}}$  can be different in different regions. However, under the same conditions, our observations suggest that the transition size  $N_{\text{trans}}$  of different nuclei within the observation window is essentially the same. The behavior of the dependence of  $N_{\text{trans}}$  on the frequency and on the amplitude of the AEF is also qualitatively consistent in the whole system. In this work, all the related quantitative measurements were conducted in the same observation window in the center of the sample.

In this system, the supersaturation necessary for crystallization is enhanced by decreasing frequency.<sup>[23]</sup> Figure 3 shows a typical structure transition at a higher degree of

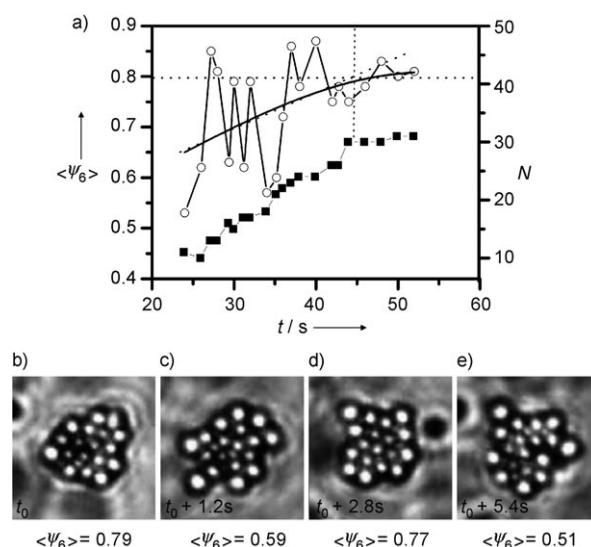


**Figure 3.** Transient crystalline structure of nuclei under conditions of  $V_{\text{pp}} = 2.5 \text{ V}$ ,  $f = 3000 \text{ Hz}$ . a)  $\langle \psi_6 \rangle$  ( $\circ$ ) and  $N$  ( $\blacksquare$ ) as a function of time. b,d) Fluctuation cause nuclei to have transient crystalline structure. c,e) Liquid-like structure displayed by precritical nuclei.

supersaturation with  $f=3000$  Hz and  $V_{pp}=2.5$  V. In contrast to the behavior of  $\langle\psi_6\rangle$  in Figure 2,  $\langle\psi_6\rangle$  in Figure 3a can be as high as 0.8 instantaneously even when it is smaller than the transition size (ca. 30). This result means that the nuclei can acquire a crystalline structure even before they reach the transition size. However, the crystalline structure of the precritical nuclei, as suggested by the substantial fluctuation of  $\langle\psi_6\rangle$  in Figure 3a, is transient. This transience can be seen more clearly from the time sequence Figure 3b–e. In Figure 3b,d, the structure of the nucleus is ordered. In the subsequent seconds (Figure 3c,e), the structure becomes disordered again. Only as the size is beyond the transition size of around 30 does the crystalline structure become stable. Experimentally, it was found that when the degree of supersaturation is enhanced further by decreasing frequency to 1000 Hz,  $\langle\psi_6\rangle$  can be as high as 0.8 from the beginning (Figure 4), and crystal nuclei are created initially with a stable crystalline structure as suggested by the CNT.<sup>[7,8]</sup>

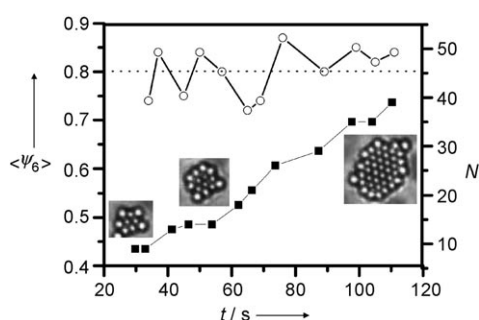


**Figure 4.** Under the condition of  $V_{pp}=2.5$  V and  $f=1000$  Hz, nuclei are created with a crystalline structure from the beginning when the degree of supersaturation is high enough.  $\circ$ :  $\langle\psi_6\rangle$ ;  $\blacksquare$ :  $N$ .

The fluctuation of the value of  $\langle\psi_6\rangle$  in Figures 2–4 is induced by thermal fluctuations. For a nucleus, the energy barrier between its metastable liquid-like structure and its stable crystal-like structure is dependent on both the degree of supersaturation and its size. At high degrees of supersaturation, when the energy difference between the metastable liquid-like structure and the stable crystal-like structure is smaller than  $k_B T$ , the thermal fluctuation can induce a global transition from the liquid-like structure to the crystal-like structure or vice versa, as we have seen in Figure 3. When the energy difference becomes larger at low degrees of supersaturation, the thermal fluctuation can induce only a local structure transition at the interface between the liquid-like fringe and the crystal-like core, giving rise to a local fluctuation of  $\langle\psi_6\rangle$  as shown in Figure 2.

The results in Figures 2–4 reveal that the initial structure of the crystal nuclei and the route of the structure evolution of the crystal nuclei are supersaturation-dependent. At low degrees of supersaturation, a metastable liquid-like structure is highly desired to occur first. The common understanding of the occurrence of a metastable structure is that the nucleation barrier for the metastable structure is much lower than that for the final stable structure.<sup>[24,25]</sup> Therefore, the nucleation of the metastable structure occurs much faster. According to the

CNT, the 2D nucleation barrier  $\Delta G_c^*$  for a crystalline nucleus is given by Equation (2).<sup>[7,8]</sup>

$$\Delta G_c^* = \frac{\pi\gamma_c^2\Omega}{\Delta\mu_c} \quad (2)$$

Here,  $\gamma_c$  is the 2D line tension of the stable crystal phase,  $\Delta\mu_c$  is the difference in chemical potential between the mother phase and the stable crystal phase, and  $\Omega$  is the average area occupied by a structure unit. However, in simulations,<sup>[11,12]</sup> it was supposed that the precritical nuclei of crystal are completely liquid-like, and a liquid-crystal structure transitions will occur sharply at the critical size. In this case, the nucleation barrier is determined by Equation (3).

$$\Delta G_l^* = \frac{\pi\gamma_l^2\Omega}{\Delta\mu_l} \quad (3)$$

Here  $\gamma_l$  is the 2D line tension of the liquid phase and  $\Delta\mu_l$  is the difference in chemical potential between the mother phase and the liquid phase. Since the liquid phase is metastable with respect to the crystalline phase, one can expect that  $\Delta\mu_l < \Delta\mu_c$ . However, because  $\Delta G^*$  is proportional to the square of  $\gamma$ ,  $\Delta G^*$  is more sensitive to the change of  $\gamma$ . Because  $\gamma_l$  is usually much smaller than  $\gamma_c$ ,  $\Delta G_l^*$  in practice should be greatly smaller than  $\Delta G_c^*$ . Nevertheless, in our experiments as shown in Figure 2, the structure transition was a continuous process in which the core of precritical nuclei becomes first crystal-like while the outer layer remains liquid-like. In this case, the nucleation barrier should be given by Equation (4).

$$\Delta G_{\text{conti}}^* = \frac{\pi\gamma_l^2\Omega}{\Delta\mu_c} \quad (4)$$

Since in a crystallizing system,  $\Delta\mu_l < \Delta\mu_c$ , then  $\Delta G_{\text{conti}}^* < \Delta G_l^*$ , which may explain why a continuous structure transition rather than a sharp structure transition occurs experimentally. However, when the degree of supersaturation is high enough, the transition size or the critical size for nuclei becomes so small that the nucleation barrier for a crystalline nucleus becomes negligible with respect to  $k_B T$ . As a consequence, nuclei can be created with a stable crystalline structure from the beginning as Figure 4 indicates.

Equations (2) and (4) suggest that to quantify the relative reduction of the nucleation barrier  $\Delta G_{\text{conti}}^*/\Delta G_c^*$ , it is necessary to determine  $\gamma_l/\gamma_c$ . However, it is a big challenge experimentally to measure  $\gamma_l$  and  $\gamma_c$  directly. As an alternative approach, these values can be derived from the experimentally determined nucleation rates and the critical sizes. In the CNT, the nucleation rate is determined by nucleation barrier  $\Delta G^*$  [Eq (5)]<sup>[7,8]</sup>

$$J = C \exp\left(-\frac{\Delta G^*}{k_B T}\right) \quad (5)$$

The radius of critical nuclei in CNT, assuming 2D disklike nuclei, is  $r^* = \gamma\Omega/\Delta\mu$ . With  $J$  and  $r^*$ ,  $\gamma$  can be determined by Equation (6).

$$\gamma = -\frac{k_B T \ln J_1 - \ln J_2}{\pi \frac{r_1^* - r_2^*}{r_1^* r_2^*}} \quad (6)$$

In Equation (6), it is assumed that  $\gamma$  is the same at different degrees of supersaturation. In our experiment, the critical size of nuclei is represented by  $N_{\text{trans}}$ .  $N_{\text{trans}}$  and the nucleation rate  $J$  were measured at different frequencies (Figure 5a). The value of  $r^*$  was determined by  $N_{\text{trans}}$  from

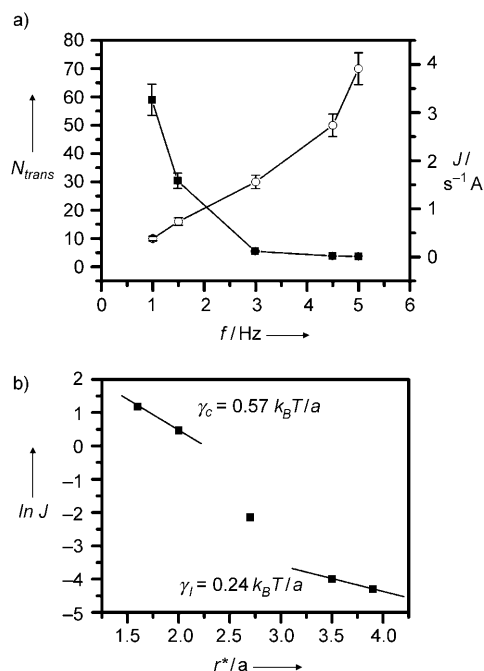


**Figure 5.** a) Experimentally measured critical transition size and nucleation rate.  $\circ$ :  $N_{\text{trans}}$ ;  $\blacksquare$ :  $J$ . b) Plot of  $\ln J$  versus  $r^*$ , from which the line tension is determined.  $a$  is the diameter of the colloidal particles.

$r^* = (N_{\text{trans}} \Omega / \pi)^{1/2}$ , and  $\Omega$  was determined from the average center–center distance  $d$  according to  $\Omega = \pi d^2/4$ . A plot of  $\ln J$  versus  $r^*$  is shown in Figure 5b. Although the interaction between colloidal particles and thus  $\gamma$  in this system are dependent on the frequency and the strength of the electric field,<sup>[21,22]</sup> in this work we assume that the interaction changes little and Equation (6) can be applied when the frequency changes are minimal, for example, from 5.0 kHz to 4.5 kHz or from 1.5 kHz to 1.0 kHz. With this assumption,  $\gamma$  was determined as  $\gamma_1 \approx 0.14 k_B T/a$  ( $a$  is the diameter of the colloidal particles) with  $J$  and  $r^*$  measured at frequencies of 5.0 kHz and 4.5 kHz, and  $\gamma$  was measured as  $\gamma_2 \approx 0.57 k_B T/a$  with  $J$  and  $r^*$  measured at frequencies of 1.5 kHz and 1.0 kHz. The value of  $\gamma_1$  is much smaller than that of  $\gamma_2$ , because the precritical nuclei at frequencies of 5.0 kHz and 4.5 kHz are characterized by a liquid-like exterior layer. Therefore,  $\gamma_1$  is actually the line tension  $\gamma_l$  of the liquid phase. However, at low frequencies, nuclei are created with a crystalline structure from the beginning as Figure 4 shows. Therefore,  $\gamma_1/\gamma_2 \approx 0.25$  can serve as an measurement of  $\gamma_l/\gamma_c$ . However, in our system, the decrease of frequency will increase the strength of the attraction between colloidal particles,<sup>[21,22]</sup> which suggests that

$\gamma_c$  at high frequencies of 5.0 kHz and 4.5 kHz should be smaller than those measured at low frequencies of 1.5 kHz and 1.0 kHz. Thus,  $\gamma_l/\gamma_c$  at high frequencies should be larger than 0.25. Given the interaction between colloidal particles,  $\gamma_l/\gamma_c$  can also be estimated roughly from the bond number. In our system, the average bond number for a 2D crystal surface particle is 4.0, whereas the average bond number for a 2D liquid-like surface particle is around 2.9, which can produce a rough estimate of  $\gamma_l/\gamma_c \approx 0.73$ . However, the bonding between two liquid-like particles is usually weaker than that between two crystal-like particles. Therefore, we should have  $\gamma_l/\gamma_c < 0.73$ . On the basis of the above discussion, we suggest that the value of  $\Delta G_{\text{cont}}^* / \Delta G_c^*$  should be 0.06–0.53, which means that the nucleation barrier at low degrees of supersaturation is significantly reduced because of the occurrence of the continuous structure transition.

In summary, the initial structure of the crystal nuclei is supersaturation-dependent. At low degrees of supersaturation, the crystal nuclei tend to nucleate with a metastable liquid-like structure and subsequently experience a continuous transition from the metastable to the final stable and crystalline-ordered structure. This route promises a nucleation barrier that is much lower than that predicted by the CNT. In other words, the gradual approach to the final stable structure can significantly facilitate the nucleation dynamics. At high degrees of supersaturation, where the nucleation barrier decreases substantially, adopting the structure of the bulk crystals during nucleation is not energetically unfavorable and then the CNT becomes valid in describing the dynamic behavior of nucleation.

The conclusions of this study are based on the observation of 2D nucleation. Thermodynamically, however, the underlying mechanism of 2D nucleation and 3D nucleation are very similar: both are dynamical processes dominated by the competition between the reduced bulk free energy and the increased interface free energy. Therefore, the conclusions obtained in this study can be logically extended to 3D nucleation.<sup>[26–28]</sup> Nevertheless, in 3D crystallization, the nucleation barrier is determined by Equation (7).

$$\Delta G^* = \frac{16 \pi \gamma^3 \Omega^2}{3 \Delta \mu^2} \quad (7)$$

Comparing Equation (7) with Equation (2), we can see that the 3D nucleation barrier is more sensitive to the change of surface tension  $\gamma$ , which implies that in 3D nucleation, a continuous structure transition is more effective in reducing the nucleation barrier.

While it offers new insight into the crystallization of colloids, the knowledge acquired in this study can also be applied to improve our understanding in protein crystallization, because it has been found that the solutions of globular proteins exhibit the similar phase behavior to colloidal suspensions.<sup>[20,29,30]</sup> We notice that there is also evidence that nucleation in atomic systems may be dominated by similar mechanisms as observed in colloidal systems.<sup>[24,29–31]</sup> However, it is necessary to point out that nucleation is essentially a kinetic process, which is, to a large extent, dominated by the nature of particle–particle interactions, the properties of

substrates, etc. Therefore, the route of nucleation may vary from system to system.

## Experimental Section

Monodisperse colloidal particles (polystyrene spheres of diameter 0.99  $\mu\text{m}$ , polydispersity < 5%, Bangs Laboratories) were dispersed uniformly in deionized water. The colloidal suspension was then sealed between two parallel horizontal conducting glass plates coated with indium tin oxide (ITO). In this system, particles in the bulk liquid are transported by the fluid flow induced by the AEF to the surfaces of the glass plates. On the surfaces of the glass plates, colloidal particles are brought together by a long-range attraction induced by the electrohydrodynamic mechanism,<sup>[21,22]</sup> and two-dimensional crystallization occurs under certain conditions. The processes of crystallization were recorded for analysis by a digital camera (CoolSNAP cf, Photometrics), which was mounted on an Olympus BX51 microscope. The interaction between colloidal particles was modified by adding  $\text{Na}_2\text{SO}_4$  at a concentration of  $2 \times 10^{-4} \text{ M}$ .

Received: September 28, 2008

Published online: January 8, 2009

**Keywords:** colloids · crystal engineering · crystal growth · nucleation

- [1] X. Y. Liu, N. Du, *J. Biol. Chem.* **2004**, 279, 6124.
- [2] H. Jiang, X. Y. Liu, *J. Biol. Chem.* **2004**, 279, 41286.
- [3] T. Baron, F. Mazen, C. Busseret, A. Souifi, P. Mur, F. Fournel, M. N. Séméria, H. Moriceau, B. Aspard, P. Gentile, N. Magnea, *Microelectron. Eng.* **2002**, 61–62, 511.
- [4] Z. L. Wang, J. Song, *Science* **2006**, 312, 242.
- [5] C. A. Mitchell, L. Yu, M. D. Ward, *J. Am. Chem. Soc.* **2001**, 123, 10830.
- [6] C. S. Towler, R. J. Davey, R. W. Lancaster, C. J. Price, *J. Am. Chem. Soc.* **2004**, 126, 13347.
- [7] D. Kashchiev, *Nucleation: Basic Theory with Applications*, Butterworth-Heinemann, Oxford, **2000**.
- [8] A. Laaksonen, V. Talanquer, D. W. Oxtoby, *Annu. Rev. Phys. Chem.* **1995**, 46, 489.
- [9] E. Ruckenstein, Y. S. Djikaev, *Adv. Colloid Interface Sci.* **2005**, 118, 51.
- [10] D. Moroni, P. R. ten Wolde, P. G. Bolhuis, *Phys. Rev. Lett.* **2005**, 94, 235703.
- [11] J. P. K. Doye, F. Calvo, *Phys. Rev. Lett.* **2001**, 86, 3570.
- [12] A. Lomakin, N. Asherie, G. B. Benedek, *Proc. Natl. Acad. Sci. USA* **2003**, 100, 10254.
- [13] P. N. Pusey, W. van Megen, P. Bartlett, B. J. Ackerson, J. G. Rarity, S. M. Underwood, *Phys. Rev. Lett.* **1989**, 63, 2753.
- [14] J. Zhu, M. Li, R. Rogers, W. Meyer, R. H. Ottewill, STS-73 Space Shuttle Crew, W. B. Russel, P. M. Chaikin, *Nature* **1997**, 387, 883.
- [15] T. H. Zhang, X. Y. Liu, *J. Phys. Chem. B* **2007**, 111, 14001.
- [16] W. Ostwald, *Z. Phys. Chem.* **1897**, 22, 289.
- [17] P. R. ten Wolde, D. Frenkel, *Phys. Chem. Chem. Phys.* **1999**, 1, 2191.
- [18] W. Poon, *Science* **2004**, 304, 830.
- [19] D. Frenkel, *Science* **2002**, 296, 65.
- [20] V. J. Anderson, H. N. W. Lekkerkerker, *Nature* **2002**, 416, 811.
- [21] F. Nadal, F. Argoul, P. Hanusse, B. Pouligny, A. Ajdari, *Phys. Rev. E* **2002**, 65, 061409.
- [22] P. J. Sides, *Langmuir* **2003**, 19, 2745.
- [23] K.-Q. Zhang, X. Y. Liu, *Nature* **2004**, 429, 739.
- [24] J. F. Lutsko, G. Nicolis, *Phys. Rev. Lett.* **2006**, 96, 046102.
- [25] A. Navrotsky, *Proc. Natl. Acad. Sci. USA* **2004**, 101, 12096.
- [26] X. Y. Liu, *J. Chem. Phys.* **1999**, 111, 1628.
- [27] X. Y. Liu, *J. Chem. Phys.* **2000**, 112, 9949.
- [28] X. Y. Liu, K. Maiwa, K. Tsukamoto, *J. Chem. Phys.* **1997**, 106, 1870.
- [29] P. R. ten Wolde, D. Frenkel, *Science* **1997**, 277, 1975.
- [30] T. H. Zhang, X. Y. Liu, *J. Am. Chem. Soc.* **2007**, 129, 13520.
- [31] K.-Q. Zhang, X. Y. Liu, *Phys. Rev. Lett.* **2006**, 96, 105701.